PERGAMON

International Journal of Heat and Mass Transfer 45 (2002) 5159–5170

International Journal of HEAT and MASS TRANSFER

www.elsevier.com/locate/ijhmt

A general model for studying effects of interface layers on thermoelectric devices performance

X.C. Xuan [a,*], K.C. Ng [a], C. Yap [a], H.T. Chua [b]

[a] *Department of Mechanical Engineering, National University of Singapore, 10 Kent Ridge Crescent, Singapore 119260, Singapore*
[b] *Bachelor of Technology Programme, Faculty of Engineering, National University of Singapore, Singapore 117576, Singapore*

Received 15 November 2001; received in revised form 14 June 2002

Abstract

Interface layers play important roles in thermoelectric (TE) devices. The present study employs a phenomenological model to study the effects of internal and/or external interface layers on TE devices performance. Sets of general performance formulae are derived for both TE coolers and generators. Some simplifications are presented, and familiar performance formulae are found by introducing effective or equivalent properties such as electrical resistivity, thermal conductivity and Seebeck coefficient. Moreover, temperature–entropy diagrams are built to understand the effects of interface layers on TE thermodynamic cycles. Together with the power-efficiency curves, TE devices performance can be fully comprehended. In addition, a popular example is analysed, and new results are presented.

1. Introduction

Recently, there has been a resurgence of interest in thermoelectric (TE) cooling and power generating devices, because they are quiet and reliable, and friendly to our environment [1–8]. A TE device generally comprises several p–n thermocouples sandwiched by two thermally conductive but electrically insulating ceramic substrates, which act as the interface layers between the device and its heat exchangers (referred to as external interface layers below). Other than the external interface layers, more interface layers usually have to be inserted into the junctions between thermoelements and metal electrodes (referred to as internal interface layers below), so that the properties degradation of TE materials can be avoided. It is definite that these interface layers will influence the transport of heat and/or electricity. For the case of a bulk TE device, the impedances resulting from internal and/or external interfaces are negligible compared to those of the device itself [11,15,16]. This neglect, however, may lead to great deviations for microdevices. Many researchers have investigated the effects of internal electrical and/or external thermal contact resistances on TE devices performance. Some simplified performance formulae were presented as functions of the length of thermoelements [9–16], but all those efforts were just incomplete analyses.

In this work a general model is established to study the effects of internal and/or external interface layers on TE devices performance. Aside from the internal electrical resistances, the internal and/or external thermal resistances are also taken into account as well as the possible internal Seebeck coefficient. Universal performance formulae are derived for both TE coolers and generators. Simplifications are performed at some specific conditions. Moreover, simple temperature–entropy (T–s) diagrams are built to deepen the thermodynamic understanding of effects of interface layers.

* Corresponding author. Tel.: +65-6874-2285; fax: +65-6779-1459.
E-mail address: mpexxc@nus.edu.sg (X.C. Xuan).

0017-9310/02/$ - see front matter
PII: S0017-9310(02)00217-X

Nomenclature

COP	coefficient of performance of coolers
E	electrical field ($V\,m^{-1}$)
g	thermoelectric arms packing density
j	dimensionless electrical current density
J, J	electrical current density ($A\,m^{-2}$)
$\mathbf{J}_q$	heat flux density circulating within devices ($W\,m^{-2}$)
$\mathbf{J}''_q$	heat flux density between devices and reservoirs ($W\,m^{-2}$)
$\mathbf{J}_s$,J_s	entropy flux density circulating within devices ($W\,m^{-2}\,K^{-1}$)
$\mathbf{J}_{s,\mathrm{tot}}$	total entropy flux density ($W\,m^{-2}\,K^{-1}$)
k	thermal conductivity ($W\,m^{-1}\,K^{-1}$)
k_i	thermal conductance per unit area of interface layers ($W\,m^{-2}\,K^{-1}$)
l	length of thermoelements
M	$\left(1+\frac{1}{2}Z(T_\mathrm{c}+T_\mathrm{h})^{1/2}\right)$
p	output power density ($W\,m^{-2}$)
q	cooling power density ($W\,m^{-2}$)
r, s, t	defined ratios
T_1, T_2	referred end temperature of thermocouples
T_c	temperature of the cold reservoir (K)
T_h	temperature of the hot reservoir (K)
x^*	dimensionless space coordinate
Z	$\alpha^2/\rho k$, figure of merit (K^{-1})

Greek symbols

α	Seebeck coefficient ($V\,K^{-1}$)
ρ	electrical resistivity ($\Omega\,m$)
ρ_i	electrical resistance per unit area of interface layers ($\Omega\,m^2$)
ε	defined constant
ε_C	COP of a reversible Carnot refrigerator
ϕ_C	reciprocal of efficiency of a reversible Carnot heat engine
σ_tot	total rate of entropy generation ($W\,m^{-3}\,K^{-1}$)
η	power conversion efficiency of power generators

Subscripts

eff	effective properties
eqv	equivalent properties
i	related to interface layers
max	maximum performance
n	related to n-type thermoelements

2. General model

A general phenomenological model is set up first to study barely the effect of internal interface layers, though, in fact, it is also suited to external interface layers. The applicability of this model in both the two types of interface layers will be clarified in the later text. One thermocouple is extracted from the TE device as displayed in Fig. 1(a), and its four internal interface layers are assumed to be identical, i.e., with similar structures and impedances. The length of interface layers is realistically far less than that of thermoelements, while their cross-sectional areas are of the same magnitude. For the simplicity, p- and n-types of thermoelements are assumed to have symmetric dimensions and properties. Moreover, we assume that thermoelements including interface layers are thermally insulated from surroundings except the heat exchanges with reservoirs. While thermal resistances of heat exchangers have been demonstrated to influence devices performance, they are omitted so as to study specially the effect of interface layers in this work [17]. All the

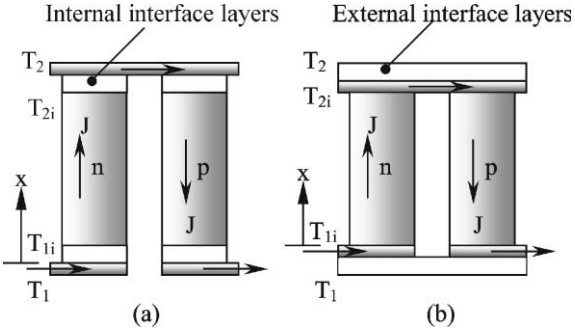

Fig. 1. A general model for a thermocouple extracted from TE devices: (a) for the case of internal interface layers; (b) for the case of external interface layers.

material properties are assumed to be independent of temperature in the currently concerned temperature range. But the impedance of metal electrodes is viewed as none.

From steady-state equations for the transport of electricity (**J**, electrical current density) and heat ($\mathbf{J}_q$, heat flux density) in a TE thermodynamic cycle [18],

$$\mathbf{J} = -\frac{1}{\rho}(\mathbf{E} + \alpha\nabla T), \tag{1}$$

$$\mathbf{J}_q = -k\nabla T + \mathbf{J}\alpha T, \tag{2}$$

one can easily get the universal energy conservation equation in an arbitrary control volume,

$$k\nabla\cdot\nabla T + \mathbf{J}\cdot\mathbf{J}\rho = 0, \tag{3}$$

where ρ, k and α are, respectively, the electrical resistivity, thermal conductivity and Seebeck coefficient of thermoelements, and **E** the electrical field.

Further relying on irreversible thermodynamics [18–22], elegant T–s diagrams have been successfully built to understand TE devices performance [23]. The unified entropy balance equation is given by

$$T\nabla\cdot\mathbf{J}_s = -\nabla\cdot\mathbf{J}_q'' + T\left[\sigma_{\mathrm{tot}} - \mathbf{J}_q''\cdot\nabla\left(\frac{1}{T}\right)\right], \tag{4}$$

$$\mathbf{J}_s = \mathbf{J}_{s,\mathrm{tot}} - \frac{\mathbf{J}_q''}{T}, \tag{5}$$

where $\mathbf{J}_{s,\mathrm{tot}}$ is the total entropy flux density, σ_{tot} the entropy source strength or the total rate of entropy generation per unit volume, $\mathbf{J}_s$ the entropy flux density circulating within a thermodynamic cycle that we intend to track, and $\mathbf{J}_q''$ the heat flux density into/out of the control volume from/to the reservoirs that one cares. The square bracketed term in Eq. (4) indicates the rate of internal entropy generation within the control volume. Using the Onsager reciprocity [18–22], $\mathbf{J}_s$ in TE devices can be derived as

$$\mathbf{J}_s = \frac{-k\nabla T}{T} + \mathbf{J}\alpha. \tag{6}$$

Along adiabatic p- and n-type thermoelements where $\mathbf{J}_q'' = 0$, Eq. (4) is reduced to

$$\nabla\cdot\mathbf{J}_s = \sigma_{\mathrm{tot}} = -k\nabla T\cdot\nabla\left(\frac{1}{T}\right) + \frac{\rho\mathbf{J}\cdot\mathbf{J}}{T}. \tag{7}$$

Therefore, the total rate of entropy generation σ_{tot} is contributed by two parts: one is the first term on the right-hand side of Eq. (7) arising from the finite-temperature-difference heat conduction, and the other is the second term associated with the Joulean heating. At the connections of thermoelements and internal interface layers, $\mathbf{J}_s$ should be continuous in the absence of thermal exchange with reservoirs. At the junctions between interface layers and metal electrodes, Eq. (4) yields $T\nabla\cdot\mathbf{J}_s = -\nabla\cdot\mathbf{J}_q''$ because no entropy is generated at the zero-volume junctions. Please note that $\mathbf{J}_q''$, here, reflects the absorbed or rejected heat flux density from/to reservoirs. Along metal electrodes, however, Eq. (6) is as simply as $\mathbf{J}_s = 0$.

Since the transportations of heat and electricity in a TE device are frequently assumed to take place in a one-dimensional space, we can easily determine the temperature distribution along each component as well as the entropy flux density $\mathbf{J}_s$, based on which the general performance formulae can be derived. Only the n-type arm of a thermocouple is analysed below due to the symmetric structure and properties of n- and p-type thermoelements. A unified space coordinate x is set up along the direction of electrical current as shown in Fig. 1(a). For the universality in TE coolers and generators, temperatures of the two metal electrodes (i.e., the temperatures of reservoirs due to the assumed zero thermal resistances of heat exchangers) are referred to as T_1 and T_2 along the current direction at the present stage. It is evident that $T_1 = T_h$ and $T_2 = T_c$ is for the case of a cooling couple, while $T_1 = T_c$ and $T_2 = T_h$ for a power generating couple. The interface temperatures T_{1i} and T_{2i} are introduced to reflect the temperature drops across the internal interface layers.

For the T_1-end interface layer: since the resistance per unit area is usually introduced to describe the effect of interface layers, we may rewrite Eqs. (3) and (6) as

$$k_i\frac{\mathrm{d}^2T}{\mathrm{d}x^{*2}} + J^2\rho_i = 0, \tag{8}$$

$$J_{s,\mathrm{i}} = -k_{\mathrm{i}}\frac{\mathrm{d}T}{\mathrm{d}x^*}\frac{1}{T} + J\alpha_{\mathrm{i}}, \tag{9}$$

where α_{i}, ρ_{i} and k_{i} are, respectively, the Seebeck coefficient, electrical resistance and thermal conductance per unit area of the interface layer, J_s the one-dimensional entropy flux density, J the one-dimensional electrical current density, and x^* the dimensionless coordinate defined as x/l_{i} with l_{i} being the assumed length of the interface layer. Note that the subscript i, below, denotes the interface layers specially. Using the boundary conditions $T(0) = T_1$ and $T(1) = T_{1\mathrm{i}}$, the distributions of T_{i} and $J_{s,\mathrm{i}}$ along the T_1-end interface layer can be expressed by

$$T_{\mathrm{i}}(x^*) = \tfrac{1}{2}J^2\rho_{\mathrm{i}}(-x^{*2} + x^*)/k_{\mathrm{i}} + (T_{1\mathrm{i}} - T_1)x^* + T_1, \tag{10}$$

$$J_{s,\mathrm{i}}(x^*) = \frac{\frac{1}{2}J^2\rho_{\mathrm{i}}(2x^* - 1) + (T_1 - T_{1\mathrm{i}})k_{\mathrm{i}}}{\frac{1}{2}J^2\rho_{\mathrm{i}}(-x^{*2} + x^*)/k_{\mathrm{i}} + (T_{1\mathrm{i}} - T_1)x^* + T_1} + J\alpha_{\mathrm{i}}. \tag{11}$$

For the n-type thermoelement: Eqs. (3) and (6) are similarly rewritten as

$$\frac{k}{l}\frac{\mathrm{d}^2T}{\mathrm{d}x^{*2}} + J^2\rho l = 0, \tag{12}$$

$$J_{s,\mathrm{n}} = -\frac{k}{l}\frac{\mathrm{d}T}{\mathrm{d}x^*}\frac{1}{T} + J\alpha_{\mathrm{n}}, \tag{13}$$

where l is the length of thermoelements, and the subscript n denotes the n-type thermoelement (note α_{n} is negative). Using the boundary conditions $T(0) = T_{1\mathrm{i}}$ and $T(1) = T_{2\mathrm{i}}$, the distributions of T_{n} and $J_{s,\mathrm{n}}$ along the thermoelement can be found as

$$T_{\mathrm{n}}(x^*) = \tfrac{1}{2}J^2\rho l^2(-x^{*2} + x^*)/k + (T_{2\mathrm{i}} - T_{1\mathrm{i}})x^* + T_{1\mathrm{i}}, \tag{14}$$

$$J_{s,\mathrm{n}}(x^*) = \frac{\frac{1}{2}J^2\rho l(2x^* - 1) + (T_{1\mathrm{i}} - T_{2\mathrm{i}})k/l}{\frac{1}{2}J^2\rho l^2(-x^{*2} + x^*)/k + (T_{2\mathrm{i}} - T_{1\mathrm{i}})x^* + T_{1\mathrm{i}}} + J\alpha_{\mathrm{n}}. \tag{15}$$

For the T_2-end internal interface layer: solving Eqs. (8) and (9) with the boundary conditions $T(0) = T_{2\mathrm{i}}$ and $T(1) = T_2$, T_{i} and $J_{s,\mathrm{i}}$ along the T_2-end interface layer can be derived as

$$T_{\mathrm{i}}(x^*) = \tfrac{1}{2}J^2\rho_{\mathrm{i}}(-x^{*2} + x^*)/k_{\mathrm{i}} + (T_2 - T_{2\mathrm{i}})x^* + T_{2\mathrm{i}}, \tag{16}$$

$$J_{s,\mathrm{i}}(x^*) = \frac{\frac{1}{2}J^2\rho_{\mathrm{i}}(2x^* - 1) + (T_{2\mathrm{i}} - T_2)k_{\mathrm{i}}}{\frac{1}{2}J^2\rho_{\mathrm{i}}(-x^{*2} + x^*)/k_{\mathrm{i}} + (T_2 - T_{2\mathrm{i}})x^* + T_{2\mathrm{i}}} + J\alpha_{\mathrm{i}}. \tag{17}$$

According to the steady-state energy conservation principle, one-dimensional heat flux density J_q in Eq. (2) should be continuous at the junctions between interface layers and the thermoelement, which thus leads to

$$J\alpha_{\mathrm{i}}T_{1\mathrm{i}} + \tfrac{1}{2}J^2\rho_{\mathrm{i}} + k_{\mathrm{i}}(T_1 - T_{1\mathrm{i}}) = J\alpha_{\mathrm{n}}T_{1\mathrm{i}} - \tfrac{1}{2}J^2\rho l + (T_{1\mathrm{i}} - T_{2\mathrm{i}})k/l, \tag{18}$$

$$J\alpha_{\mathrm{i}}T_{2\mathrm{i}} - \tfrac{1}{2}J^2\rho_{\mathrm{i}} + k_{\mathrm{i}}(T_{2\mathrm{i}} - T_2) = J\alpha_{\mathrm{n}}T_{2\mathrm{i}} + \tfrac{1}{2}J^2\rho l + (T_{1\mathrm{i}} - T_{2\mathrm{i}})k/l. \tag{19}$$

The interface temperatures $T_{1\mathrm{i}}$ and $T_{2\mathrm{i}}$ can then be found as

$$T_{1\mathrm{i}} = \frac{[T_1(1+t) + T_2t] - jtT_1(1-s) + \frac{1}{2Z}j^2t(1+r)[1+2t-jt(1-s)]}{(1+2t) - (jt)^2(1-s)^2}, \tag{20}$$

$$T_{2\mathrm{i}} = \frac{[T_1t + T_2(1+t)] + jtT_2(1-s) + \frac{1}{2Z}j^2t(1+r)[1+2t+jt(1-s)]}{(1+2t) - (jt)^2(1-s)^2}, \tag{21}$$

where $j = J\alpha l/k$, $s = \alpha_{\mathrm{i}}/\alpha_{\mathrm{n}}$, $r = \rho_{\mathrm{i}}/(\rho l)$ and $t = k/(k_{\mathrm{i}}l)$ are all dimensionless parameters, and the last three reflect the effect of impedance of interface layers. In turn, the temperature distributions in Eqs. (10), (14) and (16) can be determined as well as the entropy flux densities in Eqs. (11), (15) and (17). Heat flux densities $J''_{q,1}$ and $J''_{q,2}$ at the T_1- and T_2-ends of the n-type TE arm are, respectively, described by

$$J''_{q,1} = J\alpha'_{\mathrm{n}}T_1 - \tfrac{1}{2}J^2\rho l\left[r + (1+r)\frac{(1+2t) - jt(1-s)}{(1+2t) - (jt)^2(1-s)^2}\right] + \frac{k}{l}(T_1 - T_2)\frac{1 - (1+\varepsilon)j^2t(1-s)^2}{(1+2t) - (jt)^2(1-s)^2}, \tag{22}$$

$$J''_{q,2} = J\alpha'_{\mathrm{n}}T_2 + \tfrac{1}{2}J^2\rho l\left[r + (1+r)\frac{(1+2t)+jt(1-s)}{(1+2t)-(jt)^2(1-s)^2}\right] + \frac{k}{l}(T_1 - T_2)\frac{1+\varepsilon j^2 t(1-s)^2}{(1+2t)-(jt)^2(1-s)^2}, \tag{23}$$

$$\alpha'_{\mathrm{n}} = \alpha_{\mathrm{n}}\left[s + \frac{1-s}{(1+2t)-(jt)^2(1-s)^2}\right], \tag{24}$$

where $\varepsilon = T_2/(T_1 - T_2)$.

3. Effect of internal interface layers on TE coolers performance

For the case that $T_1 = T_{\mathrm{h}}$ and $T_2 = T_{\mathrm{c}}$, the above thermocouple is operated as a cooler. According to Eqs. (22) and (23), general formulae for its cooling power density q (positive here, expressed by the cooling power density q_{n} of the n-type arm. If the area of the cold-end metal electrode is $2g$ times the cross-sectional area of thermoelements, the actual cooling power density of a TE cooler should be q_{n}/g. In this work, g is assumed to be unity) and coefficient of performance (COP) can be easily obtained as

$$q = -J\alpha'_{\mathrm{n}}T_{\mathrm{c}} - \tfrac{1}{2}J^2\rho l\left[r + (1+r)\frac{(1+2t)+jt(1-s)}{(1+2t)-(jt)^2(1-s)^2}\right] - \frac{k}{l}(T_{\mathrm{h}} - T_{\mathrm{c}})\frac{1+\varepsilon_{\mathrm{C}} j^2 t(1-s)^2}{(1+2t)-(jt)^2(1-s)^2}, \tag{25}$$

$$\mathrm{COP} = \frac{q}{-J\alpha'_{\mathrm{n}}(T_{\mathrm{h}} - T_{\mathrm{c}}) + J^2\rho l\left[r + (1+r)\dfrac{1+2t}{(1+2t)-(jt)^2(1-s)^2}\right] + \frac{k}{l}(T_{\mathrm{h}} - T_{\mathrm{c}})\dfrac{(1+2\varepsilon_{\mathrm{C}})j^2 t(1-s)^2}{(1+2t)-(jt)^2(1-s)^2}} \tag{26}$$

with $\varepsilon_{\mathrm{C}} = T_{\mathrm{c}}/(T_{\mathrm{h}} - T_{\mathrm{c}})$ being the COP of a Carnot refrigerator. Consequently, the electrical resistances of internal interface layers degrades TE coolers performance certainly, while the interface Seebeck coefficients can improve the performance only if $s > 0$. As to the thermal resistances of interface layers, it is difficult to make a straightforward estimation, because they reduce both the Peltier and conduction heats but increase the Joule heat.

One can note that the electrical resistances of internal interface layers will limit the acceptable current level to be no higher than the maximum current density for an ideal thermocouple in the absence of interface layers, i.e., the current density at the maximum cooling power referred to as $\alpha T_{\mathrm{c}}/(\rho l)$ where $\alpha = -\alpha_{\mathrm{n}}$. As a result,

$$jt = \frac{J\alpha l}{k}t \leqslant \frac{\alpha^2 T_{\mathrm{c}}}{\rho k}t = (ZT_{\mathrm{c}})t, \tag{27}$$

where $Z = \alpha^2/(\rho k)$ is the so-called figure of merit of TE materials. Due to the limit of material properties, ZT_{c} is about unity at best to date. The dimensionless ratio $t = k/(k_{\mathrm{i}} l)$, however, is strongly dependent on the length of thermoelements. Today, k is about 1.5–2 W m^{-1} K^{-1} for the most popular room temperature TE materials, while k_{i} can attain 10^5 W m^{-2} K^{-1} in modern fabrication technology. Therefore, we propose the following three-region processing approach with regard to different l.

For bulk TE coolers [12] *or* $l \geqslant 500$ μm: since $jt < 0.04 \ll 1$, Eqs. (25) and (26) can be reduced to

$$q = -J\alpha_{\mathrm{eff}}T_{\mathrm{c}} - \tfrac{1}{2}J^2\rho_{\mathrm{eff}}l - k_{\mathrm{eff}}(T_{\mathrm{h}} - T_{\mathrm{c}})/l, \tag{28}$$

$$\mathrm{COP} = \frac{q}{-J\alpha_{\mathrm{eff}}(T_{\mathrm{h}} - T_{\mathrm{c}}) + J^2\rho_{\mathrm{eff}}l}, \tag{29}$$

where the effective TE properties are, respectively, defined as $\alpha_{\mathrm{eff}} = \alpha_{\mathrm{n}}(1+2st)/(1+2t)$, $\rho_{\mathrm{eff}} = \rho(1+2r)$ and $k_{\mathrm{eff}} = k/(1+2t)$. Clearly, Eqs. (28) and (29) are similar to those of ideal TE coolers without interface impedances. So we can freely use the ideal formulae by replacing all the properties with their corresponding *effective* values. At this time, the effective figure of merit is expressed by

$$Z_{\mathrm{eff}} = Z\frac{(1+2st)^2}{(1+2r)(1+2t)}. \tag{30}$$

It is evident that Z_{eff} is less than Z unless $s \geqslant (\sqrt{1+2t}-1)/(2t)$, e.g., $s \geqslant 0.49$ at $t = 0.03$. As Z governs the maximum temperature difference and COP of TE coolers directly, the thermal resistances will lower the two maxima unless $s \geqslant (\sqrt{1+2t}-1)/(2t)$. Other than Z_{eff}, the maximum cooling power is still dependent on k_{eff} which is decreased by the

thermal resistances of interface layers, so we have to consider the effect of thermal resistances on q at specific operation conditions.

For bulk microcoolers [12] *or* $500 > l \geqslant 100$ μm: since $(jt)^2 < 0.04 \ll 1$, Eqs. (25) and (26) may be reduced to

$$q = -J\alpha_{\text{eff}}T_{\text{c}} - \tfrac{1}{2}J^2\rho_{\text{eff}}\left[1 + (1+r)\frac{jt(1-s)}{(1+2r)(1+2t)}\right]l - \frac{k_{\text{eff}}}{l}(T_{\text{h}} - T_{\text{c}})\left[1 + \varepsilon_{\text{C}}j^2t(1-s)^2\right], \tag{31}$$

$$\text{COP} = \frac{q}{-J\alpha_{\text{eff}}(T_{\text{h}} - T_{\text{c}}) + J^2\rho_{\text{eff}}l + \frac{k_{\text{eff}}}{l}(T_{\text{h}} - T_{\text{c}})(1 + 2\varepsilon_{\text{C}})j^2t(1-s)^2}. \tag{32}$$

Similar estimations to those for bulk TE coolers can be made, here. Though somewhat complicated, it is still available to obtain the analytic solutions at the three extrema discussed above.

For thick and thin film microcoolers [12,14,15] *or* $l < 100$ μm: No explicit simplifications can be made at this region of l, though Ju and Ghoshal pointed that Eq. (28) could already have predicted the maximum temperature difference with reasonable accuracy [15]. Anyhow, we can conclude that at shorter l, the effect of interface layers on TE coolers performance is more significant.

The q–COP curves are shown in Fig. 2(a) for a thin film TE microcooler with and without interface layers impedances. Approximate solutions from Eqs. (28) and (29) are also shown for a comparison. It is clear that the simplified formulae cannot well approximate to the actual cooling power density and COP at least for the case of thick and thin film microcoolers. Shown in Fig. 2(b) are the T–s diagrams at a specific current density as highlighted in Fig. 2(a). The cooling power density is greatly reduced due to the effect of interface layers, which can be easily identified from the area

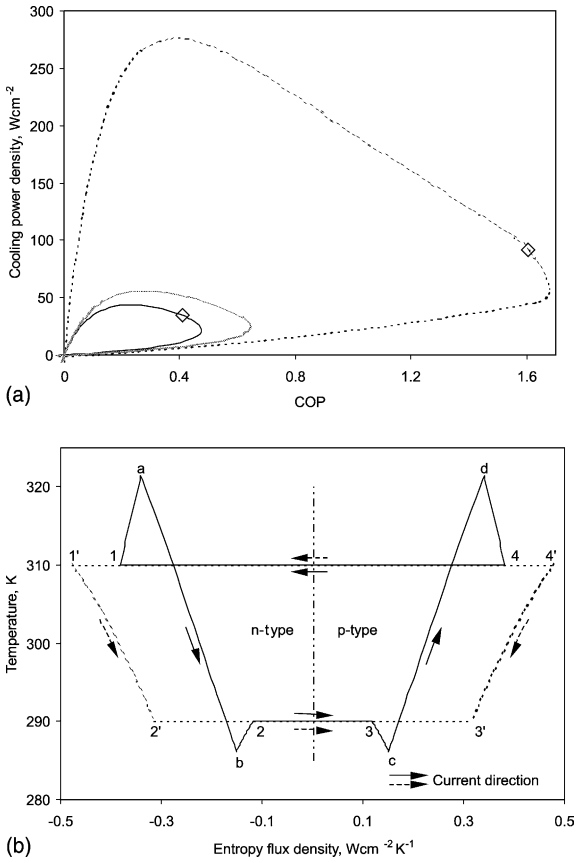

Fig. 2. Illustrations of the effect of internal interface layers on TE coolers performance: (a) q–COP; (b) T–s at $J = 30$ A mm^{-2}. The dashed-line denotes ideal coolers without interface layers impedances, while the black solid-line denotes the opposite situation. The grey solid-line in (a) represents the simplified solutions from Eqs. (28) and (29). The two points highlighted in (a) indicate the operation modes in (b). Parameters used in calculations: $T_{\text{h}} = 310$ K, $T_{\text{c}} = 290$ K, $l = 50$ μm, $\alpha = 200$ μV K^{-1}, $\rho = 10^{-5}$ Ω m, $k = 1.5$ W m^{-1} K^{-1} [24], $\alpha_{\text{i}} = 0$, $\rho_{\text{i}} = 100$ Ω μm^2, $k_{\text{i}} = 10^5$ W m^{-2} K^{-1} [15].

difference beneath the straight lines 2–3 and 2′–3′. The degradation of COP can be understood from the difference of ratio of areas beneath the lines 2–3 to 1–4 relative to that beneath lines 2′–3′ to 1′–4′, but it is much less obvious than from Fig. 2(a). We know that a peak temperature will appear in thermoelements when the electrical current exceeds a critical value [23], where ideal TE coolers are operated at the mode of maximum temperature difference. When the effect of interface layers should be accounted for, however, not only a peak temperature but also a valley temperature will arise right at the junctions between interface layers and thermoelements. This phenomenon can be understood from the points labelled by a–d in Fig. 2(b).

4. Effect of internal interface layers on TE generators performance

By analogy to the preceding section about TE coolers analysis, general formulae for the output power density p and power conversion efficiency η of a TE generator can be determined from Eqs. (22) and (23),

$$p = -J\alpha_n'(T_h - T_c) - J^2\rho l\left[r + (1+r)\frac{1+2t}{(1+2t)-(jt)^2(1-s)^2}\right] - \frac{k}{l}(T_h - T_c)\frac{(2\phi_C - 1)j^2t(1-s)^2}{(1+2t)-(jt)^2(1-s)^2}, \tag{33}$$

$$\eta = \frac{p}{-J\alpha_n'T_h - \frac{1}{2}J^2\rho l\left[r + (1+r)\frac{(1+2t)+(jt)(1-s)}{(1+2t)-(jt)^2(1-s)^2}\right] + \frac{k}{l}(T_h - T_c)\frac{1-\phi_C j^2t(1-s)^2}{(1+2t)-(jt)^2(1-s)^2}}, \tag{34}$$

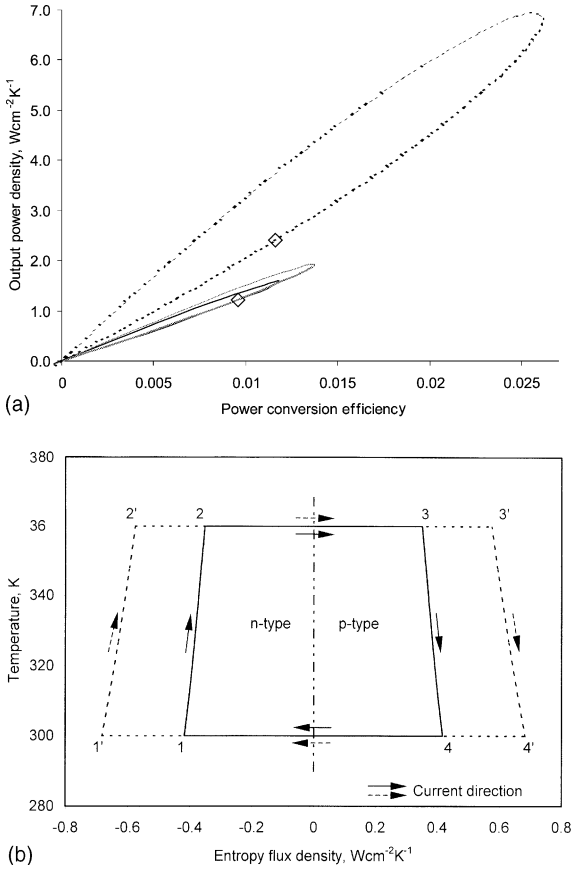

Fig. 3. Illustrations of the effect of internal interface layers on TE generators performance: (a) p–η; (b) T–s at $J = 2$ A mm^{-2}. The dashed-line denotes ideal generators without interface layers impedances, while the black solid-line denotes the opposite situation. The grey solid-line in (a) represents the simplified solutions from Eqs. (36) and (37). The two points highlighted in (a) indicate the operation modes in (b). Parameters used in calculations: $T_h = 360$ K, $T_c = 300$ K, $l = 50$ μm, $\alpha = 220$ μV K^{-1}, $\rho = 1.27 \times 10^{-5}$ Ω m, $\alpha_i = 0$, $k = 1.60$ W m^{-1} K^{-1} [24], $\rho_i = 100$ Ω μm^2, $k_i = 10^5$ W m^{-2} K^{-1} [15].

where $\phi_C = T_h/(T_h - T_c)$ is the reciprocal of efficiency of a Carnot heat engine. Since $\phi_C > 1$, p is definitely decreased due to the effect of internal interface layers. As for η, however, it should be considered at specific operation conditions, because the denominator of the right-hand side of Eq. (34) may be decreased, too.

The acceptable current density for such a TE generator is no higher than $\alpha(T_h - T_c)/(2\rho l)$, which is the current density for an ideal generator operating at the maximum p mode, so that

$$jt = \frac{J\alpha l}{k}t \leqslant \frac{\alpha^2(T_h - T_c)}{2\rho k}t = \frac{Z(T_h - T_c)}{2}t. \tag{35}$$

It seems reasonable to assume that $jt \ll 1$ is satisfied for TE generators at a relatively long l, because $Z(T_h - T_c)/2$ should be generally no higher than ZT_c. Therefore, simplified formulae like Eqs. (28) and (29) may be given,

$$p = -J\alpha_{eff}(T_h - T_c) - J^2\rho_{eff}l, \tag{36}$$

$$\eta = \frac{p}{-J\alpha_{eff}T_h - \frac{1}{2}J^2\rho_{eff}l + k_{eff}(T_h - T_c)/l}. \tag{37}$$

The curves of p vs. η are shown in Fig. 3(a) for a thin film TE generator with and without interface layers impedances. This generator has the same structure as the microcooler taken in the preceding section. There still exist obvious deviations between the simplified and complete solutions. Consequently, complete solutions should be employed in order to predict micro TE devices performance well. Shown in Fig. 3(b) are the T–s diagrams at a specific current density as highlighted in Fig. 3(a). Just like an ideal generator, no peak or valley temperature occurs in either the interface layers or thermoelements. Both the absorbed and rejected heat densities of the present generator are lowered from the areas under lines 2–3 and 4–1, respectively, compared to those under 2′–3′ and 4′–1′, so does the output power density reflected by the area difference. The power conversion efficiency η is degraded, which can be known from Fig. 3(a), but difficult to judge from Fig. 3(b). Therefore, we can conclude, now, that TE devices performance can be fully understood from the two curves of power-efficiency and T–s.

5. Effect of external interface layers

In this section, we demonstrate that the present model is also applicable to the study of the effect of external interface layers on TE devices performance. A thermocouple with external interface layers is shown schematically in Fig. 1(b). Unlike the above internal interface layers, the electrical current does not go through the external interface layers. Therefore, only the finite-rate heat transfer across these layers needs to be taken into account. As to the entropy flux density $\mathbf{J}_s$, we consider barely its circulation along with the electrical current. Eqs. (14) and (15) are still achievable. Eqs. (18)–(24) are, however, received so long as ρ_i and α_i or r and s are set zero. As a consequence, the cooling power density and COP of TE coolers are determined by

$$q = -J\alpha_n T_c \frac{1}{1 + 2t - (jt)^2} - \frac{1}{2}J^2\rho l \frac{1 + 2t + jt}{1 + 2t - (jt)^2} - \frac{k}{l}(T_h - T_c)\frac{1 + \varepsilon_C j^2 t}{1 + 2t - (jt)^2}, \tag{38}$$

$$\mathrm{COP} = \frac{q}{-J\alpha_n(T_h - T_c)\dfrac{1}{1 + 2t - (jt)^2} + J^2\rho l \dfrac{1 + 2t}{1 + 2t - (jt)^2} + \dfrac{k}{l}(T_h - T_c)\dfrac{(1 + 2\varepsilon_C)j^2 t}{1 + 2t - (jt)^2}}. \tag{39}$$

And the output power density and power conversion efficiency of TE generators are expressed by

$$p = -J\alpha_n(T_h - T_c)\frac{1}{1 + 2t - (jt)^2} - J^2\rho l \frac{1 + 2t}{1 + 2t - (jt)^2} - \frac{k}{l}(T_h - T_c)\frac{(2\phi_C - 1)j^2 t}{1 + 2t - (jt)^2}, \tag{40}$$

$$\eta = \frac{p}{-J\alpha_n T_h \dfrac{1}{1 + 2t - (jt)^2} - \frac{1}{2}J^2\rho l \dfrac{1 + 2t + jt}{1 + 2t - (jt)^2} + \dfrac{k}{l}(T_h - T_c)\dfrac{1 - \phi_C j^2 t}{1 + 2t - (jt)^2}}. \tag{41}$$

If one assumes that $jt \ll 1$ is always reasonable at different l for whether TE coolers or generators, similar formulae to Eqs. (28), (29) and (36), (37) can be, respectively, derived except the replacement of all the *effective* properties with corresponding *equivalent* properties. These equivalent properties are, respectively, defined as: $\alpha_{eqv} = \alpha_n/(1 + 2t)$, $\rho_{eqv} = \rho$ and $k_{eqv} = k/(1 + 2t)$. We have compared the simplified solutions with the complete performance formulae for a TE cooler. The results indicate that only at relatively long l and small t can the simplified solutions well approximate to the real values [16].

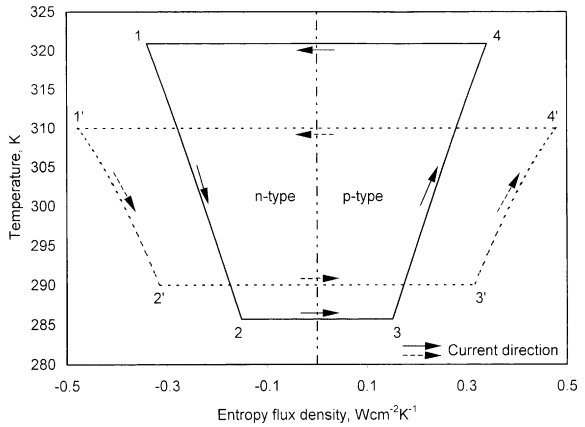

Fig. 4. Illustration of the effect of external interface layers on TE coolers performance. The dashed-line denotes ideal coolers without interface layers impedances, while the solid-line denotes the opposite situation. $J = 30\ \mathrm{A\,mm^{-2}}$ is chosen for both the two cases. Parameters used in calculations are similar to those in Fig. 2.

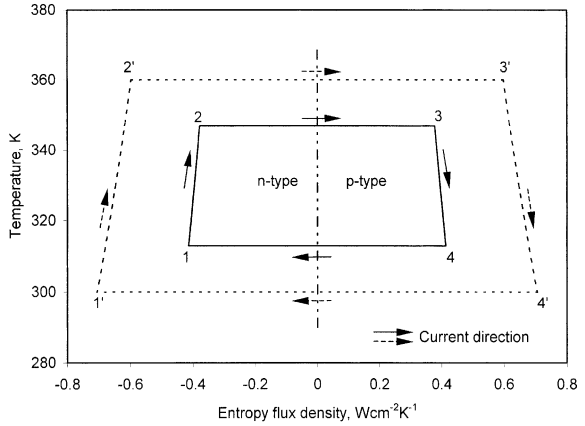

Fig. 5. Illustration of the effect of external interface layers on TE generators performance. The dashed-line denotes ideal generators without interface layers impedances, while the solid-line denotes the opposite situation. $J = 3\ \mathrm{A\,mm^{-2}}$ is chosen for both the two cases. Parameters used in calculations are similar to those in Fig. 3.

Shown in Figs. 4 and 5 are the T–s diagrams of TE coolers and generators with and without external interface layers impedances, respectively. Compared with an ideal one, the cooler itself absorbs heat at a lower temperature while rejects heat at a higher temperature due to the effect of interface layers. In other words, there exist irreversible losses across the external interface layers, which result in the cooling performance degradation. For the case of TE generators, however, the situation is right the opposite. It is still the entropy generations across the interface layers that lead to the generating performance degradation.

6. An example: mutual effects of internal and external interface layers

According to the literature, the mutual effects of electrical resistances of internal interface layers and thermal resistances of external interface layers are usually considered on TE device performance [9–15]. In this section it is also chosen as an example, and new results are presented.

Substituting $s = 0$ and $t = 0$ into Eqs. (25) and (26), and then incorporating Eqs. (38) and (39), we can obtain TE coolers performance formulae for the present case,

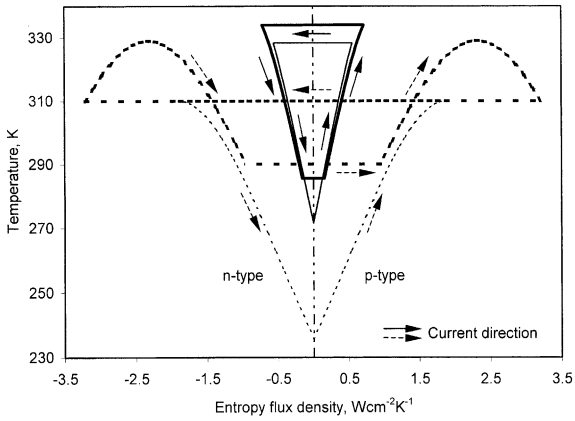

Fig. 6. Illustration of the mutual effects of internal and external interface layers on TE coolers performance. The dashed-lines denote ideal coolers without the mutual effects, of which the thicker is for the operation mode of maximum cooling power and the thinner for maximum temperature difference. The solid-lines denote coolers with the mutual effects, of which the thicker is for the mode of maximum cooling power and the thinner for maximum temperature difference. Parameters used in calculations are similar to those in Fig. 2.

$$q = -J\alpha_n T_c \frac{1}{1+2t-(jt)^2} - \tfrac{1}{2}J^2\rho l\frac{(1+2r)(1+2t+jt)}{1+2t-(jt)^2} - \frac{k}{l}(T_h - T_c)\frac{1+\varepsilon_C j^2 t}{1+2t-(jt)^2}, \tag{42}$$

$$\mathrm{COP} = \frac{q}{-J\alpha_n(T_h - T_c)\dfrac{1}{1+2t-(jt)^2} + J^2\rho l\dfrac{(1+2r)(1+2t)}{1+2t-(jt)^2} + \dfrac{k}{l}(T_h - T_c)\dfrac{(1+2\varepsilon_C)j^2 t}{1+2t-(jt)^2}}. \tag{43}$$

One can find that Eqs. (42) and (43) are, respectively, identical to Eqs. (25) and (26) at $s = 0$, which indicates that the present mutual effects are equivalent to those of internal interface layers with zero interface Seebeck coefficient. But please be noted that their thermodynamic processes are fairly different, which can be identified from Figs. 2(b) and 6. If we assume that $jt \ll 1$ is always satisfied (of course, it is more reasonable at relatively long thermoelements), Eqs. (42) and (43) reduce to

$$q = -J\alpha_{eqv}T_c - \tfrac{1}{2}J^2\rho_{eff}l - k_{eqv}(T_h - T_c)/l, \tag{44}$$

$$\mathrm{COP} = \frac{-J\alpha_{eqv}T_c - \tfrac{1}{2}J^2\rho_{eff}l - k_{eqv}(T_h - T_c)/l}{-J\alpha_{eqv}(T_h - T_c) + J^2\rho_{eff}l}. \tag{45}$$

So the maxima of the temperature difference $\Delta T = T_h - T_c$, q and COP can be, respectively, derived as

$$\Delta T_{max} = \frac{\tfrac{1}{2}ZT_c^2}{(1+2r)(1+2t)}, \tag{46}$$

$$q_{max} = \frac{k}{l}\left(\frac{\tfrac{1}{2}ZT_c^2}{(1+2r)(1+2t)} - \Delta T\right)\frac{1}{1+2t}, \tag{47}$$

$$\mathrm{COP}_{max} = \frac{M_{eqv}T_c - T_h}{(1+M_{eqv})(T_h - T_c)}, \tag{48}$$

$$M_{eqv} = \sqrt{1 + \frac{\tfrac{1}{2}Z(T_c + T_h)}{(1+2r)(1+2t)}}. \tag{49}$$

Similarly, maximum performance formulae of TE generators can be approximated by

$$p_{max} = \frac{k}{l}\frac{Z(T_h - T_c)^2}{4(1+2r)(1+2t)^2}, \tag{50}$$

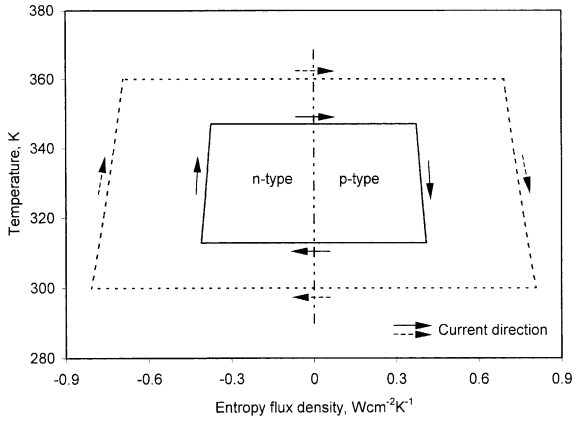

Fig. 7. Illustration of the mutual effects of internal and external interface layers on TE generators performance at the operation mode of maximum efficiency. The dashed-line denotes ideal generators without the mutual effects, while the solid-line denotes the opposite situation. Parameters used in calculations are similar to those in Fig. 3.

$$\eta_{\max} = \frac{(M_{\mathrm{eqv}} - 1)(T_{\mathrm{h}} - T_{\mathrm{c}})}{(M_{\mathrm{eqv}} + 1)T_{\mathrm{h}} - (T_{\mathrm{h}} - T_{\mathrm{c}})}. \tag{51}$$

Shown in Fig. 6 are the T–s curves of a TE cooler with and without the mutual effects of interface layers, which is operated at maximum temperature difference and maximum cooling power, respectively. Those for a TE generator operated at maximum η are displayed in Fig. 7. Obviously, the performances of TE devices are greatly diminished.

7. Conclusions

The external interface layers enables TE devices to work, while the internal interface layers stabilize TE devices performance. Their impedances, however, may influence devices performance. In the present work, a general model has been built to study the effects of internal and/or external interface layers on TE devices performance. Sets of general performance formulae have been derived for both TE coolers and generators. At some specific conditions, simplifications are presented. By introducing *effective* or *equivalent* properties, similar formulae to those of ideal TE devices are found. Only at relatively long thermoelements, however, can the simplified solutions closely follow the actual values. Complete solutions should be employed in order to predict the micro devices performance well. In addition, TE devices performance can be fully understood from the two curves of power-efficiency and T–s. The latter can help understanding the "micro" thermodynamic process, while the former tells us the "macro" devices performance.

Acknowledgements

X.C. Xuan gratefully acknowledges the financial support from The National Science and Technology Board of Singapore.

References

[1] H.J. Goldsmid, Electronic Refrigeration, Pion, London, 1986.
[2] D.M. Rowe, CRC Handbook of Thermoelectrics, CRC Press, Boca Raton, FL, 1994.
[3] F.J. Disalvo, Thermoelectric cooling and power generation, Science 285 (1999) 703.
[4] G.D. Mahan, Good thermoelectrics, in: Solid State Physics, vol. 51, Academic Press, New York, 1998, p. 81.
[5] G.D. Mahan, B. Sales, J. Sharp, Thermoelectric materials: new approaches to an old problem, Phys. Today 50 (1997) 42.
[6] C.B. Vining, Semiconductors are cool, Nature 413 (2001) 577.
[7] R. Venkatasubramanian, E. Siivola, T. Colpitts, B. O'Quinn, Thin-film thermoelectric devices with high room-temperature figures of merit, Nature 413 (2001) 597.

[8] X.C. Xuan, Analyses of the performance and polar characteristic of two-stage thermoelectric coolers, Semicond. Sci. Tech. 17 (2002) 414.
[9] Gao Min, D.M. Rowe, Cooling performance of integrated thermoelectric microclooler, Solid-State Electron. 43 (1999) 923.
[10] Gao Min, D.M. Rowe, F. Volklein, Integrated thin film thermoelectric cooler, Electron. Lett. 34 (1998) 222.
[11] Gao Min, D.M. Rowe, Improved model for calculating the coefficient of performance of a Peltier module, Energy Convers. Mgmt. 41 (2000) 163.
[12] J.P. Fleurial, A. Borshchevsky, M.A. Ryan, W. Philipps, E. Kolawa, T. Kacisch, R. Ewell, Thermoelectric microcoolers for thermal management applications, in: Proceedings of the 16th International Conference on Thermoelectrics, Dresden Germany, 1997, p. 641.
[13] V. Semeniouk, J.P. Fleurial, Novel high performance thermoelectric microcoolers with diamond substrates, in: Proceedings of the 16th International Conference on Thermoelectrics, Dresden, Germany, 1997, p. 683.
[14] U. Ghoshal, Y.S. Ju, A. Miner, M.B. Ketchen, Advanced electronic microcoolers, in: Proceedings of the 18th International Conference on Thermoelectrics, Baltimore, MD, USA, 1999, p. 113.
[15] Y. Sungtaek Ju, U. Ghoshal, Study of interface effects in thermoelectric microrefrigerators, J. Appl. Phys. 88 (2000) 4135.
[16] X.C. Xuan, Investigation of thermal contact effect on thermoelectric coolers, Energy Convers. Mgmt., (2003) in press.
[17] X.C. Xuan, Optimum design of a thermoelectric device, Semicond. Sci. Tech. 17 (2002) 114.
[18] H.B. Callen, Thermodynamics, Wiley, New York, 1960.
[19] H.B. Callen, The application of Onsager's reciprocal relations to thermoelectric, thermomagnetic, and galvanomagnetic effects, Phys. Rev. 73 (1948) 1349.
[20] C.A. Domenicali, Irreversible thermodynamics of thermoelectricity, Rev. Mod. Phys. 26 (1954) 237.
[21] S.R. De Groot, P. Mazur, Non-Equilibrium Thermodynamics, North-Holland, Amsterdam, 1962.
[22] D. Kondepudi, I. Prigogine, Modern Thermodynamics, Wiley, England, 1998.
[23] H.T. Chua, K.C. Ng, X.C. Xuan, C. Yap, J.M. Gordon, Temperature–entropy formulation of thermoelectric thermodynamic cycles, Phys. Rev. E 65 (2002) 056111.
[24] Http://www.melcor.com homepage of MELCOR, USA.